Investigation into the Morphology and Mechanical Properties of Melt-Drawn Filaments from Uncompatibilized Blends of Polystyrene and High-Density Polyethylene

Zeena Cherian,[1] Richard Lehman,[1] Kenneth VanNess[2]

[1]*AMIPP Advanced Polymer Center, School of Engineering, Rutgers University, 607 Taylor Road, Piscataway, New Jersey 08854-8065*
[2]*Department of Physics, Washington and Lee University, Lexington, Virginia*

ABSTRACT: Uncompatibilized immiscible blends of polystyrene (PS) and high-density polyethylene (HDPE) were melt-processed in a single-screw extruder fitted with a fine screen mesh and capillary die and were further drawn into filaments to produce near-nanoscale immiscible domains. The resultant morphologies and mechanical properties were studied for these structures in which load transfer is achieved solely by mechanical linkages between blend domains. The morphology of the blends revealed co-continuity approximately in the range of 45–47 volume percent PS. The development of a three-dimensional co-continuous network in 45 vol% PS, as revealed by morphology observations, was also related to a decrease in extruder output rate in this region, an indicator of the melt interaction of the two phases as co-continuity is achieved. Image analysis revealed submicron fibrillar structures near the phase inversion composition where domain sizes ranged from 6–220 nm with an average domain size of 90 nm. Tensile modulus increased with increasing PS content ($E = 2.7$ GPa at 47% PS) over the entire blend range with values greater than the rule of mixtures up to 50% PS. Strain to failure did not seem to be influenced by co-continuous morphologies and the fine dispersion of PS domains appears to constrain the fundamentally high strain of HDPE. © 2006 Wiley Periodicals, Inc. J Appl Polym Sci 103: 1616–1625, 2007

Key words: mechanical properties; immiscible blends; co-continuity; morphology; extrusion

INTRODUCTION

Many industries make use of polymer blends in order to obtain certain desired mechanical and physical properties of the finished products. Most polymer blends are immiscible and the desired properties are frequently achieved by the use of special compatibilizing additives, although a growing industry exists to produce uncompatibilized immiscible polymer blend materials for railroad ties, bridge elements, and other structural applications. Immiscible blends form a two-phase system and shape and dimensions of the dispersed phase frequently determine the properties of the blend. Abundant literature exists on the formation of dispersed (droplet/matrix) morphologies.[1–5] In recent years, much research has been focused on immiscible polymer blends with co-continuous morphologies. Co-continuity is defined as the morphological state that exists when both immiscible components are fully continuous throughout the blend system.[6] Studies have shown that the co-continuity of an immiscible polymer blend exists in a narrow range that is defined by the polymer viscosity and volume fraction.[7–11] Willemse et al.[12] have shown that co-continuous structures can also exist within a range of compositions and are influenced by interfacial tension, viscosity, and shear rate. Furthermore, studies on injection-molded materials have shown that such co-continuous blends possess good load transfer between phases due to mechanical interlocking of the two phases and these blends demonstrate approximately rule-of-mixtures properties.[13,14]

Additional improvements in properties can be anticipated by processing of finer morphologies of phases. Evstatiev et al.[15] reported studies in the melt-drawing of filaments from immiscible blends of polyethylene terephthalate/polyamides to produce microfibrillar-reinforced composites where chemical linkages arising from transreaction improve the mechanical properties. Min et al.[16] studied the rheological properties of polystyrene/polyethylene (PS/PE) filaments produced

through a capillary rheometer. In the present study we sought to generate nanoscale domains in melt-processed uncompatibilized immiscible polymer blends to assess the performance of these structures with regard to load-deformation behavior. Compatibilized blends often possess low modulus viscoelastic structures linking the two phases that are detrimental to creep properties in structural applications.[17] If rule-of-mixtures properties can be achieved exclusively via mechanical linkages, i.e., ''mechanical grafting,'' the superior creep-resistant structural composites can be developed without adding compatibilizers. Thus, the primary objective of this study was to process blends of PS and high-density polyethylene (HDPE) without compatibilizing additives by melt-drawing into filaments with near-nanoscale domains and some degree of continuity, and to assess the resultant morphologies and load-deformation behavior. The study was designed to achieve near-nano phase morphologies by melt blending two polymers in an extruder followed by extrusion through a capillary die and subsequent drawing of the extrudate to produce filaments with fine fibrillar morphology.

The formation of filaments by melt drawing requires a high degree of shear and elongational deformation of the viscous melt to reduce the dimension of the molten polymer from the die orifice size to the final filament diameter. This process is strongly dependent on the rheology of the melt, and the rheology of neat polymers was investigated in depth to define the phase inversion point. When immiscible polymers are melt blended as a two-phase liquid system in an extruder, each liquid phase responds quasi-independently to the applied stresses. In the present study, PS and HDPE with closely matched viscosities and their blends were melt-spun together over a wide range of blending ratios. Similar viscosity polymers having a viscosity ratio close to unity were chosen to achieve a minimize stress and flow differential between the phases and with the concern that drawing dissimilar viscosity materials could result in fluid instabilities within the nascent filament that would cause the filament to break and thus limit the diameter of filaments possible in this system.[18]

EXPERIMENTAL

HDPE (Chevron-Phillips, The Woodlands, TX, Marlex HHM 5202 BN) with a density of 0.951 g/cc and a melt flow index of 0.35 g/10 min at 190°C/2.16 kg was combined with general-purpose atactic polystyrene (Dow Chemical, Midland, MI, Styron 695) with a density of 1.04 g/cc and an melt flow index (MFI) of 1.5 g/10 min at 200°C/5 kg. Nine blend samples were prepared by blending the HDPE with 20, 40, 45, 47, 50, 52, 55, 60, and 80% of PS by volume. The blend compositions were selected based on the

assumption that the phase inversion point would be near 50/50 composition. Hence, more blend samples were made near this point, such as 45, 47, 50, 52, and 55 vol% PS, to better define this region. Filaments were produced by melt-drawing from these blends and also from both homopolymers.

Melt-drawing of filaments

A computer-controlled plastic processing device equipped with a single-screw extruder having an L/D ratio of 30 : 1 and a 19 mm diameter screw with a compression ratio (ratio of relative channel depth, feed section to metering sections) of 3 : 1 (C.W. Brabender Instruments, South Hackensack, NJ, Intellitorque plasticorder, extruder, and components) was used to prepare the immiscible blends. The processing temperature was 210°C for all zones. The rotational speed of the screw was maintained at 5 RPM. A spot-welded composite screen pack with a mesh screen sequence of 20/200/20 and a breaker plate was installed between the end of the screw and the die. The screen-pack was backed by a breaker plate, a disc of sturdy metal with numerous through-holes that served in this configuration as a support for the screens. A fine screen mesh served to improve mixing and homogenization of blends by increasing backpressure, to assist in the fine dispersion of phases, and also to promote elimination of bubbles.

After passing through the screen pack, the molten polymer blend exited the extruder via a round capillary die of 1 mm diameter with an L/D ratio of 30 : 1. After emerging from the die the extrudate was drawn into thin filaments using a variable speed take-up hub. The hub speed was adjusted to achieve filament diameters in the range of 100–120 μm. Although finer filaments could be made from blends, particularly at high PS levels, 100 μm was the minimum filament thickness that could be made continuously from neat HDPE without frequent rupturing. Hence, the speed was set to obtain filaments in the range of 100–120 μm for the entire composition range so that comparisons would be made on filaments of the same size. An attempt was made to produce finer filaments by extruding through a 0.5 mm die, but melt fracture prevented the extrudate from being drawn consistently into filaments, apparently due to high shear stresses at the entrance of the die.

Rheological characterization

The rheological properties of PS and HDPE were measured using an AR-2000 Rheometer (TA Instruments, New Castle, DE). Specimens were oscillated in shear using parallel plate geometry of 25 mm diameter with the gap between the plates set to 1 mm. The

frequency sweep experiments were performed at a strain rate of 1.25% in a frequency range of 100–0.01 Hz at 190–230°C at an increment of 10°C. The experiments were performed in a nitrogen atmosphere to avoid degradation of the samples. The Cox-Merz transformation rule was applied to the dynamic viscoelastic data to obtain shear viscosity as a function of shear rate.[19] A stress correction factor was also applied since the geometry used was parallel plate. In order to calculate the zero-shear viscosities of neat polymers at 190, 200, 210, 220, and 230°C, frequency sweep experiments were conducted on individual specimens. The zero-shear viscosities (η_0) for PS and HDPE were obtained by fitting the viscosity curves using Carreau and Cross viscosity models[20,21] using TA Instruments data analysis software.

Mechanical testing

The tensile properties of drawn filaments were performed on MTS Q Test/25 interfaced with a computer running MTS Test Works software for operation and data analysis. A load cell of 5N was used coupled with spring-loaded grips suitable for testing filaments. A gage length of 75 mm and crosshead speed of 50 mm/min was selected. The filament specimens were adhesive mounted on a rectangular paper template to facilitate specimen handling and mounting and also to maintain a constant gage length. The two sides of the template were snipped before testing.

An average of 10 specimens was calculated for each sample. Young's modulus was calculated from the initial linear region of the stress–strain curve. The ultimate tensile strength and breaking strain were determined at the position of rupture.

Morphology of filaments

For morphology examination, filaments were mounted in epoxy and fractured in liquid nitrogen perpendicular to the machine direction. In order to provide positive identification of both phases in the blends, the PS phase was removed by a novel etching/leaching. To achieve the necessary PS removal without collapsing the filament, the fractured specimens were held over toluene vapors for a few hours but not immersed in the liquid. Micrographs of filament morphology along the filament axis were obtained using scanning electron microscopy (SEM) and field emission SEM (FESEM) (Leo-Zeiss Gemini 982, Thornwood, NY). The samples were sputter-coated with gold-palladium for enhanced conductivity and imaging. Some of the micrographs collected from the SEM work were analyzed with image analysis software (Image J, NIH, Bethesda, MD) to determine feature size and distribution.

RESULTS AND DISCUSSION

Melt-drawing of blends

The drawability of HDPE was greatly improved by the addition of PS in amounts as small as 15–20%. The extensional behavior of 100% HDPE resin was inferior compared to PS in that little strain hardening occurred and unstable elongational strain rates were encountered which, at best, produced uncontrolled variability in the filament diameter and at worst resulted in filament failure during drawing. This behavior was also reported by Min et al.,[16] where they observed that addition of HDPE to PS leads to reduced elongation at break during extensional viscosity measurements of blends leading to unstable drawing. The phenomenon of strain hardening in polymers[22,23] is critical to stable filament drawing operations since strain-hardened materials exhibit a strong resistance against fast stretching of polymer melts, which in turn imparts draw rate stability. Thus, when neat HDPE was spun, the molten strand showed severe necking instabilities after emerging from the die and subsequent rupture of filaments occurred. On the other hand, PS filaments exhibited excellent stability and could be spun continuously due to the higher melt strength of this polymer. In blends of the two polymers, PS induces strain-hardening behavior of HDPE by acting as a high-melt strength polymer that resists extensional flow.

Viscoelastic behavior

HDPE and PS are two quite different polymers from the perspective of rheological properties, an important consideration in formulating composite blends. In the formulation phase of this work, polymer types were selected based on the simple but useful MFI parameter. The similarities in MFI suggested that both polymers would behave similarly at process temperatures and that such similarities would yield a co-continuous blend composition near the 50/50 blend, as predicted by the empirical relation given by Jordhamo et al.,[8] Paul and Barlow,[10] and Miles and Zurek.[11]

$$\frac{\eta_A}{\eta_B} = \frac{\phi_A}{\phi_B} \qquad (1)$$

where η and ϕ are the viscosity and volume fraction, respectively, of blend components A and B at the shear rate and temperature of the process.

To some degree the MFI data served as a good predictor. However, a large variation in shear viscosity was observed in PS over the temperature range of 190–230°C, while HDPE showed little variation over this temperature range, as illustrated in Figure 1(a,b). This was further exemplified by the flow activation energies calculated using standard software (TA Instruments Rheology Advantage) wherein an
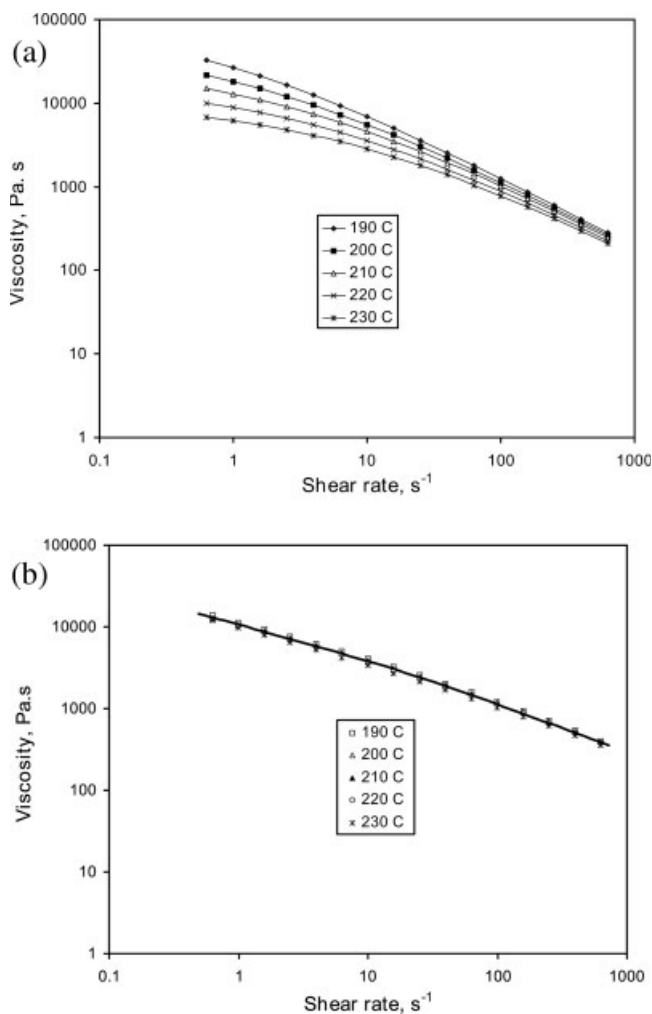
Figure 1 (a) Viscosity shear rate behavior of polystyrene at temperatures near the processing range. (b) Viscosity shear rate behavior of HDPE at temperatures near the processing range. Note insensitivity to temperature.

activation energy of 21 kJ/mole was calculated for HDPE, while PS calculations produced 114 kJ/mole. This factor of approximately five between the two activation energies indicates that the viscosity of PS is much more temperature-dependent than for HDPE.[24] The effect of shear on the viscosity of these polymers is also quite different. The zero shear viscosities (η_0), shown in Table I, based on Carreau

TABLE I
Zero-Shear Viscosity Data for the HDPE and PS Materials

Temperature [°C]	Carreau model		Cross model	
	HDPE	PS	HDPE	PS
190	14540	33160	30500	57470
200	13770	20950	28890	33320
210	13580	13880	29520	20600
220	13470	9101	31330	12860
230	13350	6080	32460	8173

and Cross models of HDPE and PS at different temperatures, show a strong dependence of viscosity on shear for PS, but nearly shear-independent behavior for HDPE, although the two models are not in complete agreement. The Carreau model gives virtually identical zero-shear viscosities at 210°C, resulting in a viscosity ratio of unity, while the Cross model gives nearly identical zero-shear viscosities at a lower temperature, ~ 203°C. Figure 2(a) shows these zero-shear viscosity curves as determined by the Cross model. The extrusion process, of course, is not a zero-shear process, and the estimated shear rate for the filament drawing methods described here is ~ 400 s^{-1}. At this shear rate the polymers behave differently, as indicated in Figure 2(b), exhibiting much lower viscosity and with nearly parallel viscosity curves. The HDPE is the higher viscosity polymer at this shear rate, $\sim 42\%$ more viscous than PS.

Examining the 400 s^{-1} data [Fig. 2(b)] suggests a phase inversion composition of 42 vol% PS. The zero-shear data, Cross model, also suggest a phase inversion composition of $\sim 40\%$ PS. However, the Carreau model shows the polymers at equal viscosity at 210°C, indicating a 50/50 phase inversion
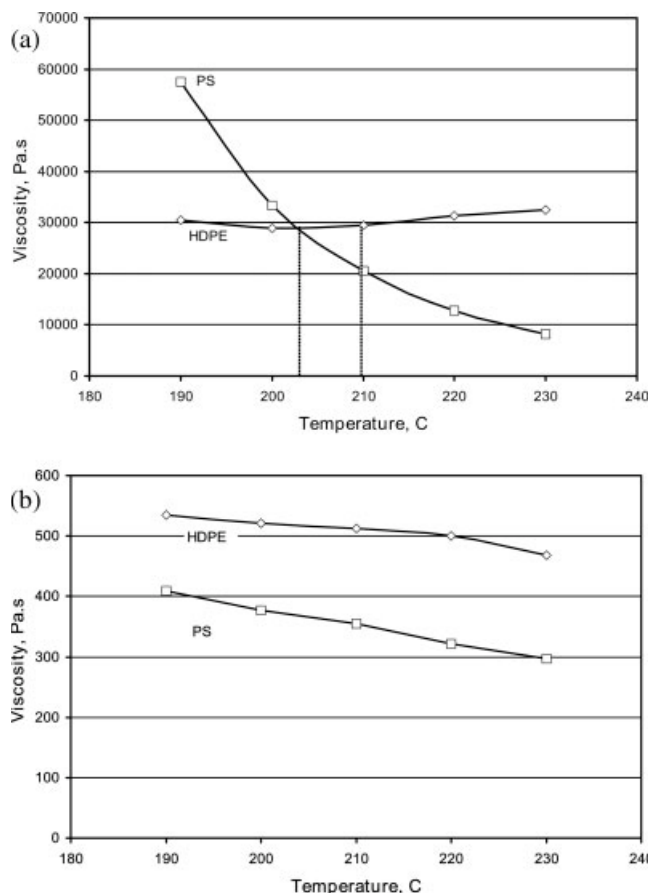

Figure 2 (a) Viscosity of HDPE and PS at zero shear. (b) Viscosity of HDPE and PS at 400 s^{-1} shear.

TABLE II
Mechanical Properties versus Composition for the Blends Studied

Volume [%]	Modulus [GPa]	Stress at yield [MPa]	Ultimate stress [MPa]	Strain at yield [%]	Strain at break [%]
100	4.19	104.8	166.0	3.7	42.2
80	3.30	68.3	111.8	3.2	32.7
60	2.74	59.7	98.3	4.8	31.6
55	2.44	55.4	82.7	7.4	29.5
52	2.55	54.2	84.5	3.8	32.6
50	2.47	55.6	78.1	6.7	26.9
47	2.70	60.2	89.2	7.9	31.4
45	2.35	54.4	80.3	8.0	28.5
40	2.42	55.5	79.6	9.2	25.9
20	1.99	43.1	56.1	5.4	17.5
0	0.98	44.0	56.7	55.9	> 500

point. Thus, for the present work it appears that an average of the Carreau and Cross models provides an effective predictor of the phase inversion composition point, even though these models are predicting zero-shear viscosities—values far from the high shear reality of extrusion. The point of phase inversion for the blends studied appears to be near 47% from the elastic modulus data discussed in the next section and near 45% based on extruder output data also subsequently discussed.

Mechanical properties

The mechanical properties measured on the filaments are shown in Table II and Figures 3–7 as a function of PS content. The modulus-composition curves (Fig. 3)

follow a nonlinear curve, with an initial region of negative curvature followed by a region of positive curvature above approximately the 50% composition point. As small amounts of PS are added to HDPE, the modulus increases at a rate greater than the rule of mixtures. This behavior continues until the 47% PS point is reached, at which time the curve falls below the rule of mixtures and remains there for all blend compositions higher in PS. The deviations from the linear relationship are modest, comprising a maximum positive deviation of +27% at 20% PS and a maximum negative deviation of −13% at 80% PS. The positive deviation at low PS concentrations may result from orientation effects in which molecular alignment enhances filament stiffness, although characterization of molecular orientation was not part of this work. As the fibers become finer near the phase inversion point, the
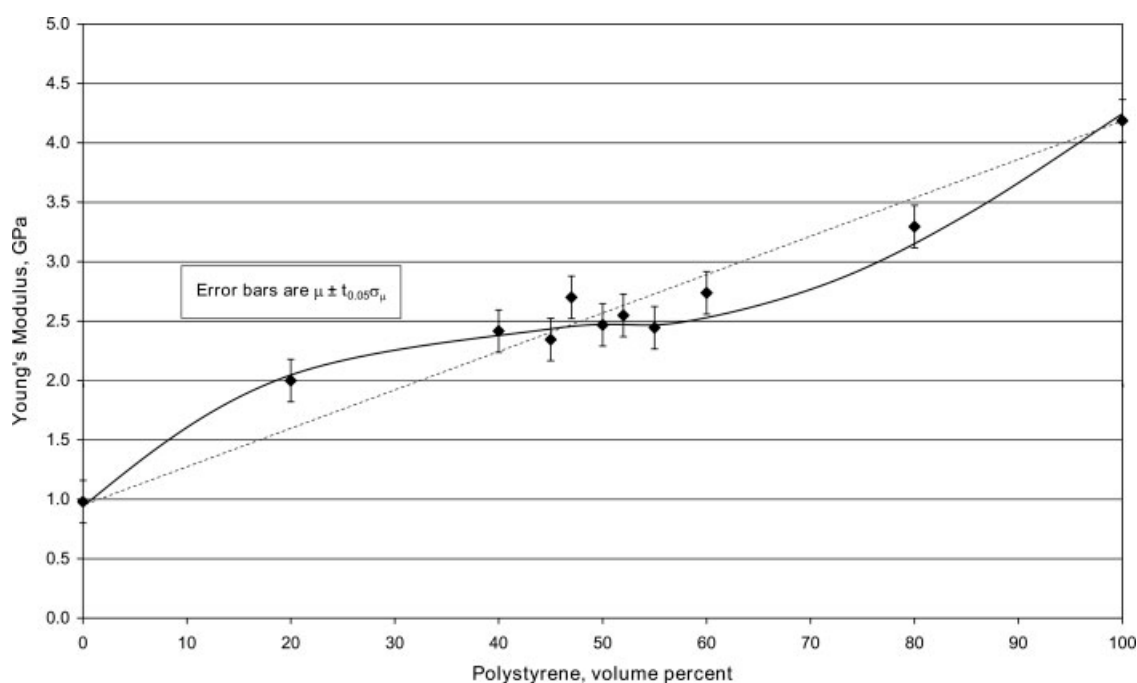

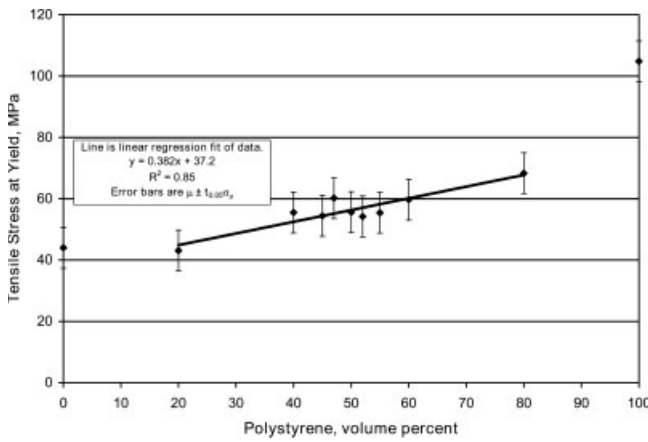**Figure 3** Modulus as a function of polystyrene content.

Figure 4 Yield stress as a function of polystyrene content.

Figure 6 Ultimate tensile strength versus polystyrene content.

amount of interfacial area increases, as does the tendency for interfacial slippage, thus lowering the load transfer effectiveness and lowering the stiffness. After the phase inversion composition, HDPE fibers exist in a PS matrix. These HDPE fibers have greater shrinkage than the PS matrix and after cooling from the melt these fibers have contracted away from the matrix. Thus, the ability of the HDPE fibers to share load with the matrix is reduced and the composite modulus reflects this occurrence. A significant result of this work is the demonstration of blend modulus values near the rule of mixtures over a wide range of compositions, a remarkable result for uncompatibilized blends of these two highly incompatible polymers.

Yield stress values for the blends followed a nearly linear relation over the blend compositions (Fig. 4), although all values were slightly below the rule-of-mixtures line defined by the yield stress of neat HDPE (44 MPa) and neat PS (105 MPa). The yield strain decreases with increasing PS concentration (Fig. 5) and again follows an approximately linear relationship. Small additions of PS (20%) greatly reduced the yield
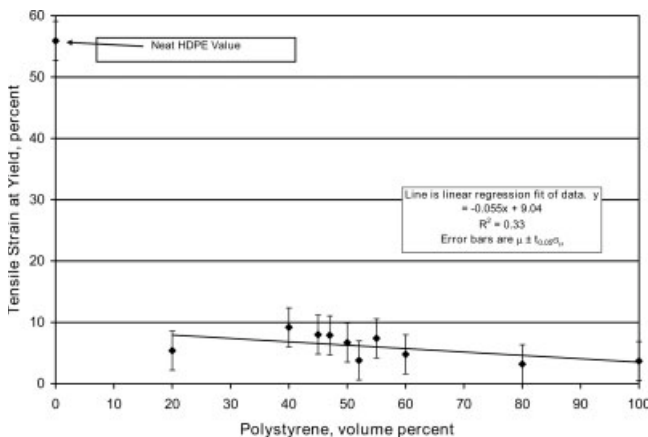
strain of the neat HDPE, from 56% to 5.4%. Apparently, the addition of finely dispersed PS interferes with the yielding mechanism of HDPE, as discussed below for a similar behavior observed for strain at failure.

The ultimate tensile strength of these filaments was below the additive values of the pure end members, PS and HDPE (Fig. 6). In the blending of the two immiscible polymers, the data clearly show that the two-phase structure is not highly efficient in load transfer and lower values result. This may result from the drawn nature of the filaments. In such drawn structures the interlocking morphology that has been observed for bulk materials[13,14] is not as prevalent, and hence interfacial slippage during tensile testing generates a translation of the line to lower values. However, in considering only the blend compositions we note the nearly linear increase in tensile strength, indicative of good mechanical interaction between the phases, with increasing PS fraction over all compositions, from 20% PS to 80% PS.

The strain-to-failure data were interesting and revealed important features of these composites. Pure
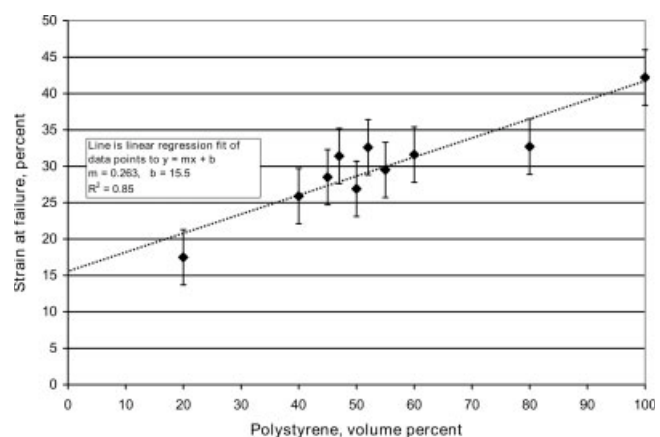

Figure 5 Yield strain as a function of polystyrene content.

Figure 7 Strain at break versus polystyrene content.

HDPE, of course, has great ductility and pure HDPE filaments failed at greater than 500% strain. Consider Figure 7, which illustrates the strain at failure for all the blend compositions. Beginning with pure PS filaments, the strain to failure (42%) begins to decrease as HDPE is added, a remarkable reversal of the usual ductility-inducing effects of HDPE. At the high PS percentage compositions, this effect is most likely due to the low modulus ''defects'' introduced into the PS structure by the dispersed HDPE. However, the continued reduction in strain to failure persists even after the phase inversion near 50% PS, and 20% PS/80% HDPE composition shows the lowest strain to failure of all blends. From these data it appears that the addition of finely dispersed PS interferes with the yielding mechanism of HDPE. Semicrystalline polymers such as HDPE display strong necking behavior and a dramatic yield point in tensile stress/strain curves. Yielding typically involves the disruption of the crystal structure and slip occurs between the crystalline lamellae and also within individual lamellae. Ordinary yielding occurs by slip at angles of about 40° to the tensile axis. As the plastic flow continues, the slip direction rotates toward the tensile axis, at which time the polymer resists further extension and lamellae and spherulites lose their identity.[25,26] The present work suggests that small amounts of finely dispersed PS in HDPE pin the structure sufficiently so that the 40° slip mechanism is disabled, which in turn reduces the yielding of blend compositions. By this mechanism, the strain to failure is reduced by at least 95% by the addition of just 20% PS. This study did not investigate compositions below 20PS/80HDPE, but the pinning effect described here may have major effects on the ductility of these composites at much lower PS concentrations. Extrapolating the dotted fit line in Figure 7 to zero PS results in an estimated ''no slip'' strain to failure of pure HDPE of just 15.5%. From the perspective of practical considerations, the important feature of the strain to failure curve is the relative maximum that occurs in the curve near the 50% composition. This is a subtle effect with regard to magnitude, and may be related to the very fine, nearly co-continuous structure that occurs at the phase inversion as revealed by microscopy and discussed below.

To provide additional information regarding the phase inversion composition, the extruder gravimetric output rate under constant operating conditions was measured. This rate (n = 3), shown in Figure 8, illustrates generally increasing output as the PS content increases, with pure PS extruding at 2.7 times the gravimetric rate of pure polyethylene. These data, which are consistent with the viscosity data at 400 sec^{-1} [Fig. 2(b),] clearly indicate that PS is the more fluid polymer under these temperature and shear rate conditions. More interesting is the behavior of the output curve at intermediate compositions. At
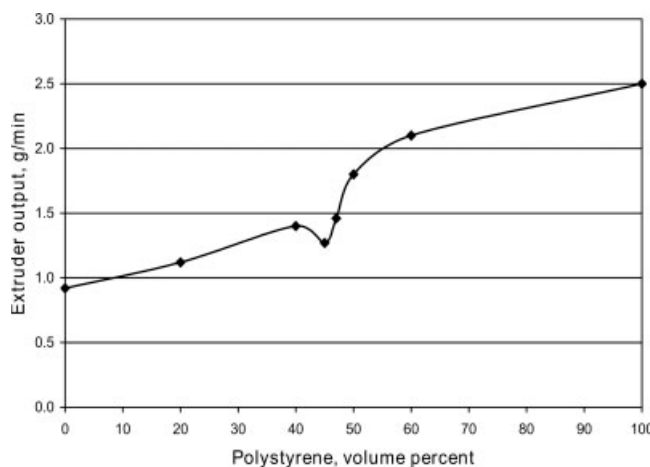

Figure 8 Output as a function of polystyrene content.

low concentrations of PS in a PE matrix, the PS is the dispersed phase and its viscosity contribution falls below the linear relationship. Likewise, at high PS concentrations the viscosity is dominated by the continuous PS phase and the relationship falls above the linear curve. Previous researchers[27–30] have suggested that the incompatible interface between immiscible polymer melts will lead to interlayer slip and a reduction in the apparent viscosity of the blend. Such a phenomenon would increase extruder output upon addition of PS, counter to the observed behavior in Figure 8, and would also generate asymmetry of the output curve about the linear relationship, also not observed. Thus, the fluid dynamics of the continuous phase appears to dominate the output behavior rather than the slip behavior between the two phases. At the phase inversion point where very fine structures, high levels of interfacial surface area, and co-continuous or nearly co-continuous structures are formed, the viscosity of the blend is expected to increase since the intertwined phases constrain the movement of each other and the blend acts as a singular phase.[8,28] In such a case the extruder output is expected to decrease at the phase inversion point. In this work such a reduction is observed at ∼ 45% PS, and this value is one data point for determining the phase inversion point in concert with mechanical property data, rheology data, and image analysis.

Morphological characterization

The morphology of extruded binary immiscible polymer blends depends principally on the relative rheology and volume fraction of the components and the degree of shear and mixing provided by the extruder. In this study, a high level of shear and domain dispersion was achieved in a single-screw extruder through the use of a 200 mesh screen pack and other processing conditions as detailed previ-
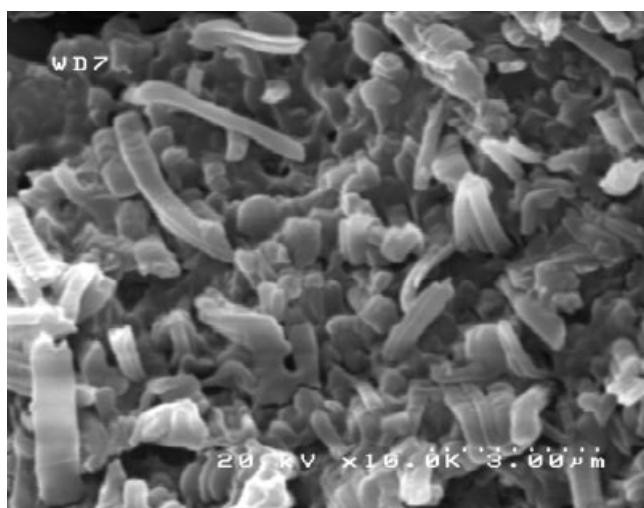
Figure 9 Pullout of polystyrene domains from HDPE matrix during cold (77 K) fracture.

ously. The morphologies of selected compositions are shown in Figures 9 and 10. The general morphology of as-fractured specimens (Fig. 9) consists principally of PS filaments pulled out of the polyethylene matrix, a common feature of filament composites in which the interfacial bonding is low. The shape of the PS pullouts illustrates a range of shapes from circular cylindrical filaments to more ribbon-like shapes. Indeed, many of the lateral PS domains consist of bundled microfilaments. The length of the pullouts reflects the degree of interfacial bonding, which in this case consists of mechanical linkages generated by the developing co-continuity of the structure.

The dark areas in Figure 10 are voids generated by the etching of PS to enhance imaging and to better reveal the morphology of both the HDPE and PS phases. The micrographs [Fig. 10(a–d)] show a fine dispersion of the phases. At 20% PS the polystyrene is clearly the dispersed phase and a high-magnification (50,000) image is shown to illustrate the discrete
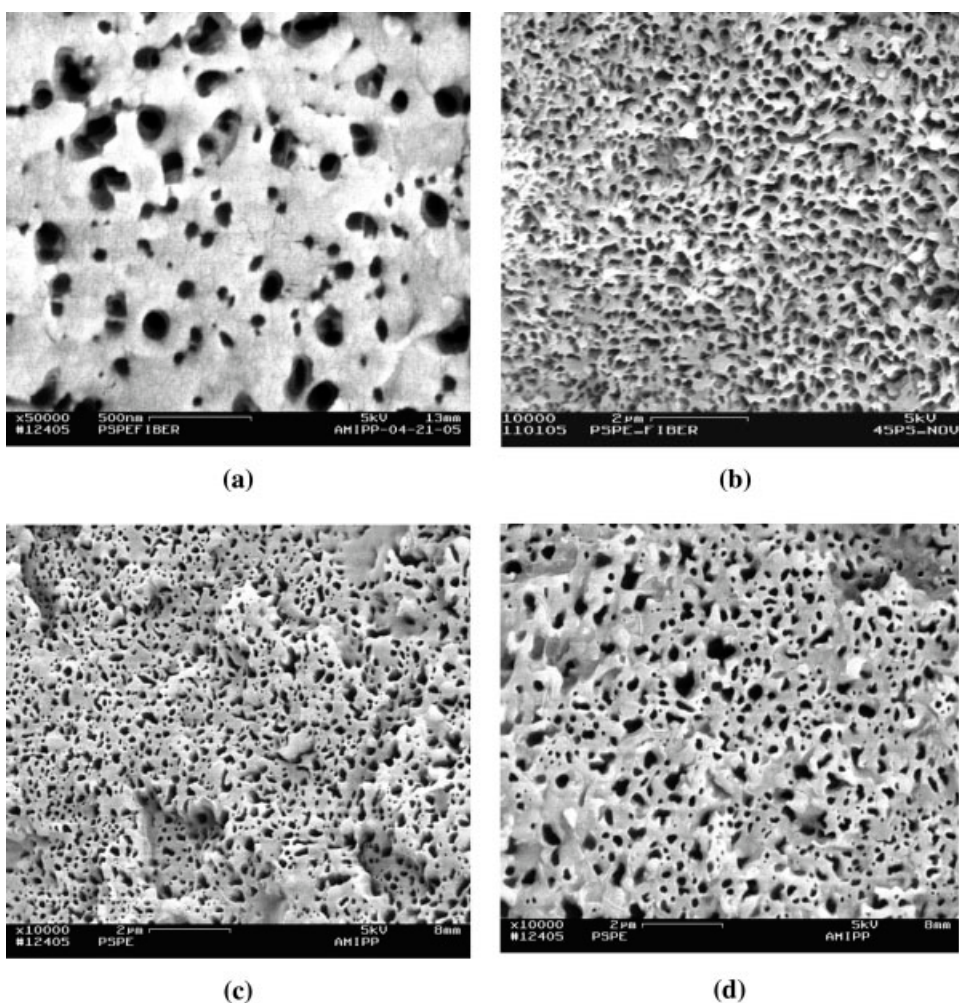

Figure 10 FESEM micrographs of PS/PE filament after removal of polystyrene phase: (a) 20PS/80HDPE; (b) 45PS/55HDPE; (c) 47PS/53HDPE; (d) 50PS/50HDPE.
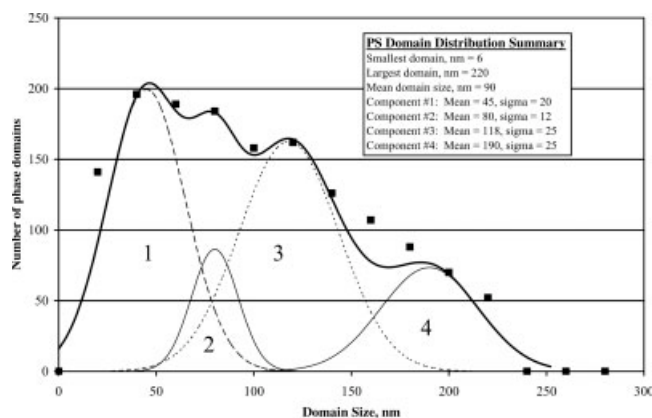
Figure 11 Polystyrene phase distribution by image analysis of 47% PS/53% HDPE composite. Approximate deconvolution of total curve illustrates normal distribution components.

nature of these domains. In the 45–47% PS sequence [Fig. 10(b–d)], a fine co-continuous type structure is seen that has been generated from the highly elongated nature of the drawn filaments.

One of the goals of this work was to assess the ability of uncompatibilized immiscible polymer blends to form small submicron domains, perhaps extending into the mesoscale region. Image analysis of the 47 vol% PS composition, considered representative of blends in this fine-scale morphology compositional range, revealed a range of small PS domains as shown in the micrograph of Figure 10 and quantified as a domain size distribution in Figure 11. The output from the image analysis software showed that the filament draw processing generates a broad range of domain sizes, ranging from 6–220 nm, with an asymmetric distribution about a mean value of 90 nm. Although the mechanisms that result in this distribution are not known and are the subject of an ongoing study, we assumed that domains arising from a single mechanism are normally distributed and thus a simple deconvolution into best-fit normal distribution components is appropriate. The result, shown in Figure 11, is the four components of the curve labeled 1–4 and comprising mean values of 45, 80, 118, and 190 nm. Thus, a mesoscale dispersion of PS in a polyethylene matrix has been achieved with an average domain size of 90 nm, which may be comprised of approximately four component distributions arising from currently undefined processing sources.

CONCLUSIONS

The phase morphology and mechanical properties of uncompatibilized blends of PS/HDPE filaments processed by melt drawing from a single-screw extruder fitted with a fine screen mesh were studied. The goal was to achieve a near-nanoscale dispersion

of phases in the blends. The predicted co-continuous composition, ~ 45% PS, was identified by measuring rheological properties of neat polymers and by calculating composition values from an empirical relationship. SEM images revealed finer domain structures and co-continuity in the range of 45–47% PS. In the 47% PS, composite polystyrene domain sizes displayed a broad size range from 6–220 nm with an average domain size of 90 nm. Deconvolution of this curve into normal distribution components suggests that the broad distribution may consist of four elements centered at 45, 80, 118, and 190 nm. From a processing perspective the region of extruder output instability was detected between 45 and 50% PS, suggesting the occurrence of phase inversion and consistent with the morphological observations. Tensile Young's modulus of all compositions increased with increasing levels of PS in HDPE, and values greater than the rule of mixtures were measured up to 47% PS content, apparently due to orientation effects. Additions of HDPE to neat PS resulted in a monotonically decreasing failure strain at all blend compositions, demonstrating the tendency of composite morphology to partially arrest the strain mechanism of HDPE.

References

1. Han, C. D. Multiphase Flow in Polymer Processing; Academic Press: New York, 1981.
2. Wu, S. Polymer 1985, 26, 1855.
3. Lee, J. K.; Han, C. D. Polymer 1999, 40, 2521.
4. Padilla-Lopez, H.; Vaquez, M. O.; Gonzalez-Nunez, R.; Rodrigue, D. Polym Eng Sci 2003, 43, 1646.
5. Guerrero, C.; Lozano, T.; Gonzalez, V.; Arroyo, E. J Appl Polym Sci 2001, 82, 1382.
6. Favis, B. D. Polymer Blends. Vol. 1: Formulation. John Wiley & Sons: New York, 2000; Chapter 16.
7. Bourry, D.; Favis, B. D. J Polym Sci B Polym Phys 1998, 36, 1889.
8. Jordhamo, G. M.; Mason, J. A.; Sperling, L. H. Polym Eng Sci 1986, 26, 517.
9. Potschke, P.; Paul, D. R. J Macromol Sci C Polym Rev 2003 C43, 1, 87.
10. Paul, D. R.; Barlow, J. W. J Macromol Sci Rev Macromol Chem 1980, C18, 109.
11. Miles, I. S.; Zurek, A. Polym Eng Sci 1988, 28, 796.
12. Willemse, R. C.; Posthuma de Boer; van Dam, J.; Gotsis, A. D. Polymer 1998, 39, 24, 5879.
13. Nosker, T. J.; Renfree, K.; VanNess, K.; Donaghy, J. J. Nature 1991, 350, 563.
14. Joshi, J.; Lehman, R. L.; Nosker, T. J. J Appl Polym Sci 2006, 99, 2044.
15. Evstatiev, M.; Schultz, J. M.; Petrovich, S.; Georgiev, G.; Fakirov, S.; Friedrich, K. J Appl Polym Sci 1998, 67, 723.

16. Min, K; White, J. L.; Fellers, J. F. J Appl Polym Sci 1984, 29, 6, 2117.
17. Bin, X.; Simonsen, J.; Rochefort, W. E. J Appl Polym Sci 1999, 76, 1100.
18. Zhang, D. F.; Zumbrunnen, D. A. J Fluid Eng 1996, 118, 40.
19. Cox, W. P.; Merz, E. H. J Polym Sci 1958, 28, 619.
20. Carreau, P. J.; Kee, D. D.; Chabra, R. P. Rheology of Polymeric Systems: Principles and Applications; Hanser: Munich, 1997.
21. Hieber, C; Chiang, H. H. Polym Eng Sci 1992, 32, 14, 931.
22. Hong, J. S.; Ahn, K. H.; Lee, S. J. Korea Aust Rheol J 2004, 16, 213.
23. Dumoulin, M. M.; Utracki, L. A.; Lara, J. Polym Eng Sci 1984, 24, 117.
24. Mackay, M. E.; Henson, D. J. J Rheol 1998, 42, 1505.
25. McCrum, N. G.; Buckley, C. B.; Bucknall, C. B. Principles of Polymer Engineering; Oxford University Press: New York, 1997.
26. Ward, I. M. Mechanical Properties of Solid Polymers; John Wiley & Sons: New York, 1983.
27. Guerrero, C.; Lozano, T.; Gonzalez, V.; Arroyo, E. J Appl Polym Sci 2001, 82, 1382.
28. Zhao, R.; Macosko, C. W. Materials Research Society Conference Proceedings, 2000, 629, FF2.1.1.
29. Bousmina, M.; Palierne, J. F.; Utracki, L. A. Polym Eng Sci 1999, 39, 1049.
30. Cohen, A.; Schroeder, R. J Rheol 1990, 34, 685.